Polyamide 6/Clay Nanocomposites Using a Cointercalation Organophilic Clay via Melt Compounding

Xiaohui Liu,[1] Qiuju Wu,[1] Lars A. Berglund,[1] H. Lindberg,[2] Jiaqi Fan,[3] Zongneng Qi[3]

[1]*Division of Polymer Engineering, Luleå University of Technology, 97187 Luleå, Sweden*
[2]*Division of Wood Material Science, Luleå University of Technology, 93187 Skellefteå, Sweden*
[3]*State Key Laboratory of Engineering Plastics, Institute of Chemistry, Chinese Academy of Sciences, Beijing, 100080, China*

Received 22 January 2002; accepted 16 September 2002

ABSTRACT: Polyamide 6/clay nanocomposites (PA6CN) were prepared via the melt compounding method by using a new kind of organophilic clay, which was obtained through cointercalation of epoxy resin and quaternary ammonium into Na-montmorillonite. The dispersion effect of this kind of organophilic clay in the matrix was studied by means of X-ray diffraction (XRD) and transmission electron microscopy (TEM); the silicate layers were dispersed homogeneously and nearly exfoliated in the matrix. This was probably the result of the strong interaction between epoxy groups and amide end groups of PA6. The mechanical properties and heat distortion temperature (HDT) of PA6CN increased dramatically. The notched Izod impact strength of PA6CN was 80% higher than that of PA6 when the clay loading was 5 wt %. Even at 10 wt % clay content, the impact strength was still higher than that of PA6. The finely dispersed silicate layers and the strong interaction between silicate layers and matrix decreased the water absorption. At 10 wt % clay content, PA6CN only absorbs half the amount of water compared with PA6. The dynamic mechanical properties of PA6CN were also studied. © 2003 Wiley Periodicals, Inc. J Appl Polym Sci 88: 953–958, 2003

Key words: polyamide 6; organophilic clay; nanocomposites

INTRODUCTION

In recent years, organic–inorganic nanocomposites have attracted great interest from researchers since they often exhibit unexpected hybrid properties synergistically derived from two components. One of the most promising composites systems would be hybrids based on organic polymers and inorganic clay minerals consisting of layered silicates.[1–25] Since synthesized polyamide 6/clay nanocomposites were first demonstrated by a group at the Toyota research center in Japan,[10–12] extensive work has been performed.

The most commonly used clay is the smectite group mineral such as montmorillonite (MMT), which belongs to the general family of 2:1 layered silicates. Their structures consist of two fused silica tetrahedral sheets sandwiching an edge-shared octahedral sheet of either aluminum or magnesium hydroxide. The silicate layers are coupled through relatively weak dipolar and van der Waals forces. The Na^+ or Ca^{2+} residing in the interlayers can be replaced by organic cations such as alkylammonium ions via an ion-exchange reaction to render the hydrophilic layered silicate organophilic.[1] Out of all of the methods to prepare polymer/clay nanocomposites, the approach based on direct melt intercalation is perhaps the most versatile and environmentally benign.

In this article, we report the preparation of PA6/clay nanocomposites (PA6CN) via melt intercalation by using a new kind of organophilic montmorillonite through cointercalation of epoxy resin and alkylammonium into Na-montmorrillonite and demonstrate their properties.

EXPERIMENT

Materials

PA6, Ultramid B3, used in this study was manufactured by BASF, and its dry properties are listed in Table I.

The cation exchange capacity (CEC) of Na-montmorillonite used in this article was 80 meq/100 g. The water content was about 7 wt % at original state [thermogravimetic analysis (TGA) method]. The particle size was less then 20 μm. Epoxy resin ARALDITE GY 240, a diglycidyl ether of bisphenol A with a molecular weight of 360, was kindly supplied by Ciba-Geigy.

The ordinary organophilic clay was prepared as the reference via an ion-exchange reaction in water using alkylammonium. One hundred grams of Na-montmorillonite was dispersed in 5000 mL of hot water using an homogenizer. Thirty grams of hexadecyl trimethyl

Correspondence to: L. A. Berglund (lars.berglund@mb.luth.se).

Journal of Applied Polymer Science, Vol. 88, 953–958 (2003)

TABLE I
Mechanical Properties and HDT of the Obtained Nanocomposites

	PA6	PA6CN5 (inorganic content 2.9 wt %)	PA6CN10 (inorganic content 5.6 wt %)	PA6/C16-MMT nanocomposite (inorganic content 5.7 wt %)
Yielding strength (MPa)	57.2	84.1 (1.44)	98.3 (1.71)	86.2 (1.51)
Tensile modulus (GPa)	2.37	4.08 (1.72)	5.04 (2.12)	4.64 (1.96)
Elongation at break (%)	133	36	9.6	5.6
Notched Izod impact strength (J/m)	64	116 (1.81)	86 (1.34)	46 (0.72)
HDT (°C) (1.82 MPa)	62	136	157	140
Flexural strength (MPa)	98.1	137.3 (1.41)	150.9 (1.53)	142.2 (1.45)
Flexural modulus (GPa)	2.41	3.33 (1.38)	4.56 (1.89)	4.14 (1.72)

The values in the parentheses are the relative values to those of PA6. The inorganic content of PA6CN5, PA6CN10, and PA6/C16-MMT nanocomposites was measured by the TGA method.

ammonium bromide was dissolved in hot water. It was poured into the Na-montmorillonite-water solution under vigorous stirring for 30 min to yield white precipitates. The precipitates were collected and washed by hot water three times, and then the precipitates were ground into the size of 20 μm after thorough drying in vacuum oven. This organophilic clay was abbreviated as C16-MMT.

The cointercalation organophilic clay was prepared as follows: 130 g C16-MMT and 20 g epoxy resin GY 240 were mixed in Haake Recorder 40 mixer for 1 h. The obtained product was abbreviated as E-MMT.

The interlayer distances of above organophilic clays and Na-montmorillonite were measured by X-ray diffraction powdery specimens.

Preparation of PA6/clay nanocomposites

A twin-screw extruder was used for preparation of the nanocomposites. PA6 granules were dried in a vacuum oven at 120°C for 24 h prior to blending with organophilic clay. The temperature of the extruder was maintained at 220, 245, 245, and 230°C from hopper to die respectively. The screw speed was maintained at 180 rpm. After drying at 80°C for 6 h, the obtained nanocomposite was injection molded to obtain specimens for measurement of tensile properties, notched Izod impact strength, heat distortion temperature (HDT), and water absorption.

Characterization

Thin films (ca. 400 μm) of the nanocomposites were prepared using various organophilic clays by hot pressing at 240°C. The films were used in X-ray diffraction (XRD) measurements to evaluate the dispersibilities of the silicate layers in the PA6 matrix. X-ray diffraction patterns of the obtained films were recorded by a Siemens D5000 X-ray diffractometer at room temperature. The CuKα radiation source was operated at 40 kV and 40 mA. Patterns were recorded by monitoring those diffractions that appeared from 1.5° to 30°. The scan speed was 2°/min. Transmission electron microscopy (TEM) observations were performed on thin sections of the injection-molded samples. A Hitachi H-800 TEM was used at an acceleration voltage of 100 kV.

Prior to testing, all specimens were dried in a vacuum oven at 80°C for 24 h. The tensile testing was carried out on a universal tensile tester (Instron 8501). The speed of crosshead for strength was 50 mm/min, while for modulus measurement was 5 mm/min. The notched Izod impact strength was measured with CS-137D-167 (Custom Scientific Instruments, Inc.) according to the respective standards. The HDT was measured following the procedure described in ASTM 648. In this work, the directions of deformation are the same with the injection axes.

The water absorption experiments were performed to provide a rough estimate of this characteristic. The molded specimens were kept in deionized, boiling water for a fixed time, and were then quickly placed between sheets of paper to remove the excess water. The amount of absorbed water was calculated from the specimen weight increase. The specimens had the following dimensions: Length 50 mm, width 12.7 mm, and thickness 3 mm.

The dynamic mechanical analysis was performed using a dynamic mechanical analyzer (Perkin-Elmer DMA-7). The testing was carried out in 3-point bending mode at a vibration frequency of 1 Hz, and a 0.2 mm amplitude sinusoidal, in a temperature range from -150 to 150°C at a heating rate of 5°C/min in a nitrogen atmosphere. The dimensions of the samples used were $10.0 \times 5.0 \times 1.5$ mm.

RESULTS AND DISCUSSION

The intercalation effect of E-MMT

Figure 1 shows the X-ray diffraction patterns of E-MMT, C16-MMT, and Na-montmorillonite, respec-

tively. Na-montmorillonite shows a characteristic diffraction peak corresponding to the (001) plane at 1.24 nm. C16-MMT shows a 1.96 nm basal space in XRD pattern. The basal space of E-MMT is 3.77 nm as shown in Figure 1. Comparing the 3.77 nm d_{001} value of E-MMT with the 1.24 nm d_{001} value of Na-montmorillonite, the increased layer distance of E-MMT demonstrates the advantage of the cointercalation organophilic clay.

The alkylammonium ion-exchange enables conversion of the hydrophilic interior clay surface to hydrophobic and increases the layer distance as well. This is the condition of C16-MMT. In this organophilic environment, epoxy resin is then diffusing into the clay galleries to increase the layer distance further. For this method applied with E-MMT, we use the term *cointercalation*.

The structure of silicate layers in PA6 matrix

Direct evidence of the intercalation is provided by the XRD patterns of the obtained hybrids. The peak of C16-MMT corresponding to the (001) plane of the silicate layers around $2\Theta = 4.5°$ is shifted to lower angle at $2\Theta = 2.2°$ for the PA6/C16-MMT nanocomposite. This corresponds to an increased silicate layer spacing from 1.96 to 3.96 nm. PA6 is intercalated between the silicate layers. The XRD pattern of PA6 nanocomposites with C16-MMT implies that the clay layers still maintain a relatively strong ordering of the layered structure.

The PA6 nanocomposites blending with 1 wt % E-MMT is abbreviated as PA6CN1; similarly, the nanocomposites having 3, 5, 7, and 10 wt % clay loading are abbreviated as PA6CN3, PA6CN5, PA6CN7, and PA6CN10, respectively. As shown in Figure 2, no peak appeared when the clay loaded less than 7 wt %. After this value, there was a small and unapparent peak, more exactly a shoulder, with a gradual increase in the diffraction intensity toward the lower angle. The lack of a sharp (001) peak in the XRD pattern indicates E-MMT has a better exfoliated effect than C16-MMT in the PA6 matrix.

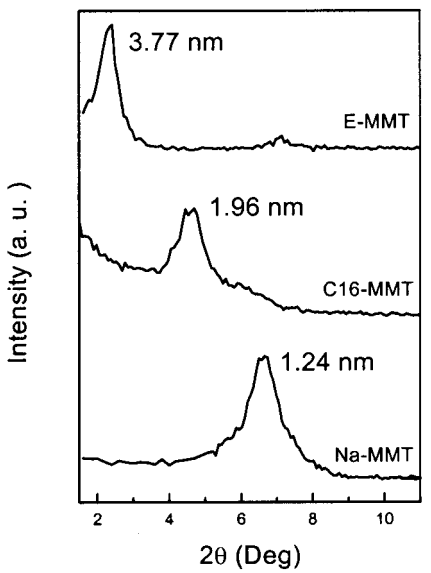

Figure 1 XRD patterns of Na-montmorillonite, C16-MMT, and E-MMT.

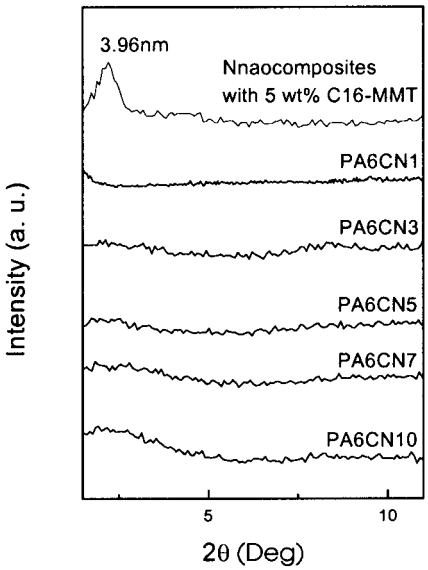

Figure 2 XRD patterns of the nanocomposite containing 5 wt % C16-MMT, PA6CN1, PA6CN3, PA6CN5, PA6CN7, and PA6CN10.

The structure of E-MMT observed by TEM is presented in Figure 3. The dark lines are the intersection of the silicate layers. One can see the layers of E-MMT are dispersed homogeneously, nearly exfoliated, in the PA6 matrix. The unapparent peak in the XRD patterns of the nanocomposites with high clay loading should be attributed to a slight amount of unexfoliated layers.

Vaia et al.[25]suggested that the confinement of the polymer inside the interlayers results in a decrease in the overall entropy of the polymer chains. At the same time, the entropic penalty of polymer confinement may be compensated by the increased conformational freedom of the tethered surfactant chains as the layers separate. But this mean-field model also indicates that the entropy associated with the aliphatic chains only increases until the tethered chains are fully extended. For the system of clay treated with hexadecyl trimethyl ammonium bromide only, the 3.96 nm basal spacing of C16-MMT dispersed in the PA6 matrix reflects the length of fully extended 16-carbon aliphatic chain. Further layer separation depends on the establishment of favorable interactions to overcome the continually increasing penalty of polymer confinement. Such intercalations must have caused the nearly exfoliated structure of PA6/E-MMT nanocomposites.

Figure 3 TEM image of PA6CN5.

First, the alkylammonium makes the silicate layers organophilic. Then the presence of epoxy end group between the layers must attract PA6 molecules and cause a strongly increased layer separation.

Mechanical properties and HDT

We prepared a series of PA6/E-MMT nanocomposites (PA6CN) with various E-MMT contents. The mechanical properties and HDT of PA6CN5 and PA6CN10 are presented in Table I as the example to illustrate the improvement in properties. The inorganic content of PA6CN5 is 2.9 wt % while that of PA6CN10 is 5.6 wt %, both of which are measured by the TGA method. The properties of the PA6/C16-MMT nanocomposite containing 5.7 wt % inorganic filler are also measured to make a comparison. The results show dramatic increases in strength, modulus, and heat resistance compared to PA6 when PA6 is compounded with E-MMT. One reason for the improvement is the presence of immobilized or partially immobilized polymer phases. Those phases have been thoroughly discussed by Eisenberg.[26] It is also likely that silicate layer orientation as well as molecular orientation contribute to the observed reinforcement effects. Compared with PA6/C16-MMT nanocomposite, the nanocomposite containing E-MMT shows a larger increase in properties, which is probably caused by the better exfoliated structure in PA6CN.

The increase in notched Izod impact strength is interesting. With previously reported polymer/clay nanocomposites, the impact strength either maintains at the same level or is lower than that of pristine like the situation showed in Table I. In this system, PA6/E-MMT nanocomposites, an 80% increase in impact strength is achieved in PA6CN5, and the impact strength of PA6CN is still higher than that of PA6 even as E-MMT content is added. The mechanism of this phenomenon needs further study.

Water absorption

It is well known that the absorption curve is represented by relationship between the amount of water absorbed in the specimen M_t and the square root of time divided by the thickness.[27] Figure 4 shows such absorption curves of PA6 and PA6CN. All curves show a nearly linear increase during the initial stage, followed by a plateau value after saturated by water. Also, Figure 5 presents the relation between the saturated water absorption amounts of PA6CN vs clay loading. The amount of water absorption in PA6CN is much less than that of PA6, and PA6CN containing 10 wt % E-MMT only absorbs half the amount of water compared with PA6. One reason must be the presence of immobilized and partially immobilized polymer in the amorphous phase. With increasing clay loading in PA6CN, the saturated water absorption amount decreases greatly before 5 wt %, after this value, the decrease in absorbed water is not so obviously. This can be attributed to the aggregation of the unexfoliated silicate layers at higher clay loading.

The diffusion coefficient D is estimated from absorption data at the early stage (1 h) using[27]

$$\frac{M_t}{M_\infty} = \left(\frac{4}{\pi^{0.5}}\right)\left(\frac{1}{\Delta X}\right)(Dt)^{0.5} \quad (1)$$

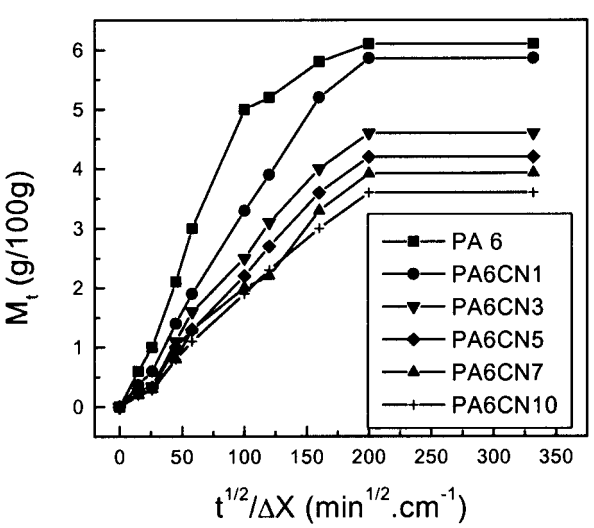

Figure 4 Water absorption curves of PA6 and PA6CN.

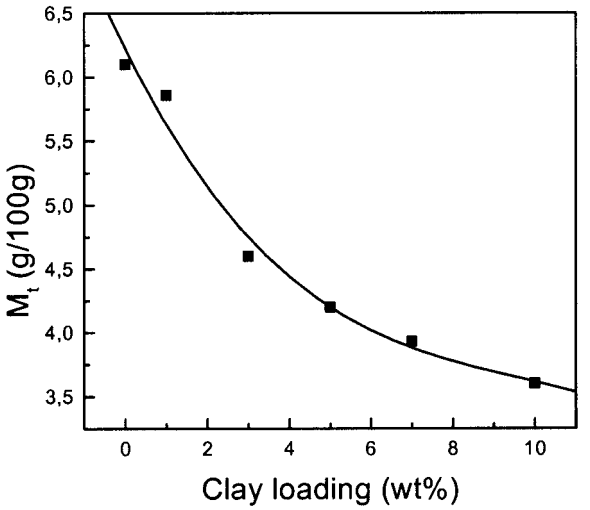

Figure 5 Dependence of water absorption amount of PA6CN on clay loading.

where ΔX is the thickness of the specimens, M_t and M_∞ are the amount of water absorbed in specimens at time t, and after an infinite time, respectively. The diffusion coefficients thus obtained are presented in Figure 6. D values decrease with an increase in the amount of E-MMT, and D for PA6CN when containing 10 wt % E-MMT is less than half of that for PA6.

In addition to the immobilized phase explanation, the presence of crystallites and impermeable particles obviously also lowers the overall rate of transport. It has also been suggested that impermeable phases increase the average diffusion path length[27]; further, the epoxy groups between silicate layers interact with the amino and amide groups of PA6. This may to some extent avoid the formation of a hydrogen bond between PA6 molecular chains and water.

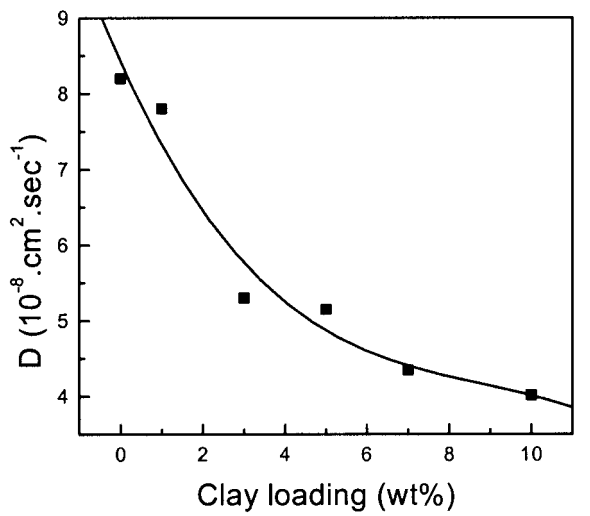

Figure 6 Dependence of D on clay loading.

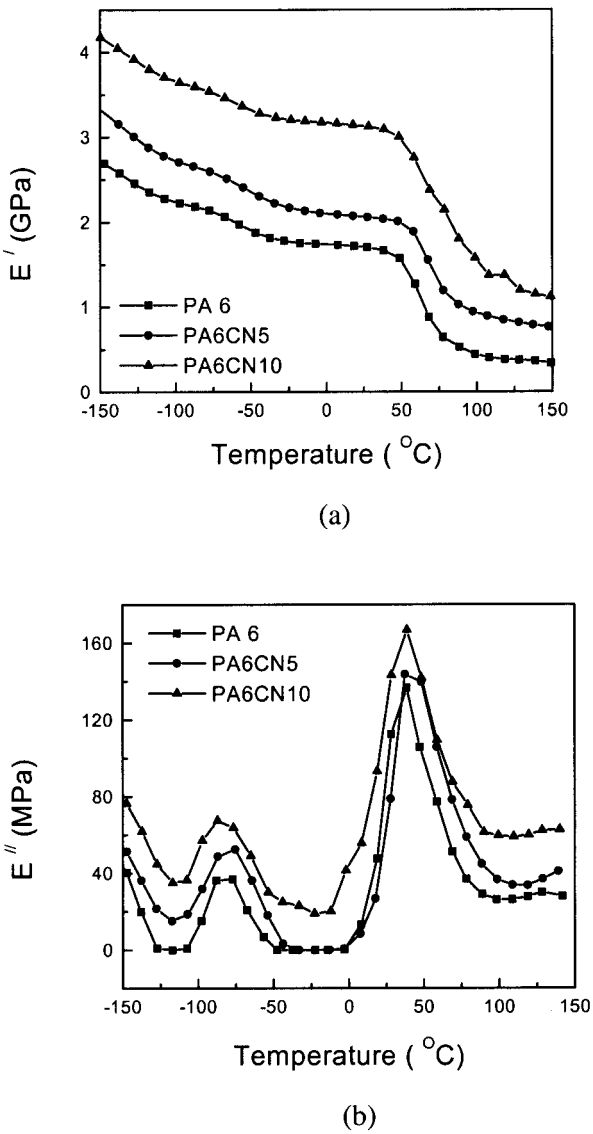

Figure 7 Dynamic mechanic spectra of PA6, PA6CN5, and PA6CN10. (a) Temperature dependence of E'. (b) Temperature dependence of E''.

Dynamic mechanical spectra of PA6CN

Dynamic storage modulus (E') and dynamic loss modulus (E'') of PA6, PA6CN5, and PA6CN10 are shown in Figure 7. In the E' curves [Fig. 7 (a)], the values of PA6CN with various E-MMT contents are higher than that of PA6 in the whole testing temperature range. In the E'' curves [Fig. 7 (b)], two relaxation peaks of the PA6 are presented. The largest peak at 50°C, T_α, is the main relaxation peak caused by the movement of large-chain segments. The peak at about −80°C is associated with the crankshaft-type motion involving the unbonded amide group and several methylene carbon groups. PA6CN has the same relaxation peaks as PA6 despite the presence of the clay.

CONCLUSION

A new kind of organophilic clay was obtained through direct melt cointercalation of epoxy resin and alkylammonium into Na-montmorillonite. PA6CN was prepared with this kind of organophilic clay by a twin-screw extruder. In this nanocomposite system, the silicate layers were dispersed homogeneously and nearly exfoliated in the PA6 matrix that was the result of the strong interaction between epoxy groups confined in the layers and amino and amide groups of PA6. The mechanical properties and HDT of PA6CN increase dramatically. It is worth noting that the notched Izod impact strength of PA6CN is higher than that of PA6, even at 10 wt % high clay content. The water absorption of PA6 was reduced by 50% as 10 wt % E-MMT was added.

References

1. Whittingham, M. S.; Jacobson, A. E. Intercalation Chemistry; Academic Press: New York, 1982.
2. Theng, B. K. G. The Chemistry of Clay Organic Reactions; Adam Hilger: London, 1974.
3. Giannelis, E. P. Adv Mater 1993, 8, 29.
4. Krishnamoorti, R.; Giannelis, E. P. Macromolecules 1997, 30, 4097.
5. Vaia, R. A.; Giannelis, E. P. Macromolecules 1997, 30, 8000.
6. Balazs, A. C.; Singh, C.; Zhulina, E. Macromolecules 1998, 31, 8370.
7. Lyatskaya, Y.; Balazs, A. C. Macromolecules 1998, 31, 6676.
8. Novak, B. M. Adv Mater 1993, 6, 422.
9. Lu, S.; Melo, M. M.; Zhao, J.; Pearce, E. M.; Kwei, T. K. Macromolecules 1995, 28, 4908.
10. Usuki, A.; Kawasumi, M.; Kojima, Y.; Fukushima, Y.; Okada, A. Kurauchi, T.; Kamigaito, O. J Mater Res 1993, 8, 1179.
11. Kojima, Y.; Usuki, A.; Kawasumi, M.; Kojima, Y.; Fukushima, Y.; Okada, A.; Kurauchi, T.; Kamigaito, O. J Mater Res 1993, 8, 1185.
12. Kojima, Y.; Usuki, A.; Kawasumi, M.; Kojima, Y.; Fukushima, Y.; Okada, A.; Kurauchi, T.; Kamigaito, O. J Polym Sci, Part A: Polym Chem 1993, 31, 1755.
13. Wang, M. S.; Pinnavaia, T. J. Chem Mater 1994, 6, 468.
14. Lan, T.; Pinnavaia, T. J. Chem Mater 1994, 6, 2216.
15. Kelly, P.; Akelah, A.; Qutubuddin, S. A. Moet, J. Mater Sci 1994, 29, 2274.
16. Vaia, R. A.; Isii, H.; Giannelis, E. P. Chem Mater 1993, 5, 1694.
17. Moet, A.; Akelah, A. Mater Lett 1993, 18, 97.
18. Messersmith, P. B.; Giannelis, E. P. J Polym Sci, Part A: Polym Chem 1995, 33, 1047.
19. Biasci, L.; Aglietto, M.; Ruggeri, G.; Ciardelli, F. Polymer 1994, 35, 3296.
20. Ogawa, M. Chem Mater 1996, 8, 1347.
21. Ruiz-Hitzky, E.; Aranda, P.; Casal, B.; Galvan, J. C. Adv Mater 1995, 7, 180.
22. Vaia, R. A.; Vasudevan, S.; Krawiec, W.; Scanlon, L. G.; Giannelis, E. P. Adv Mater1995, 7, 154.
23. Oriakhi, C. O.; Nafshan, R. L.; Lerner, M. W. MRS Bull 1996, 31, 1513.
24. Friedlander, H. Z.; Frink, C. R. Polym Lett 1964, 2, 475.
25. Vaia, R. A.; Jandt, K. D.; Kramer, E. J.; Giannalis, E. P. Macromolecules 1995, 28, 8080.
26. Tsagaropoulos, G. ; Eisenberg, A. Macromolecules 1995, 28, 6067.
27. Kojima, Y.; Usuki, A.; Kawasumi, M.; Okada, A.; Kurauuchi, T.; Kamigaito, O. J Appl Polym Sci 1993, 49, 1259.